

Direct hadron production in ultrarelativistic heavy ion collisions.

D.Yu.Peressounko, Yu.E.Pokrovsky

Russian Research Center "Kurchatov Institute", 123182 Moscow, Russia.

Abstract

Hadrons emitted by the pre-surface layer of quark-gluon plasma (QGP) before phase transition into hadronic gas are considered as possible source of direct information about QGP. It is shown that these hadrons dominate at soft p_t if QGP is created in ultrarelativistic heavy ion collisions.

PACS code: 25.75.-q

Keywords: heavy ion collisions, quark-gluon plasma.

arXiv:hep-ph/9704386v2 24 Apr 1997

1 Introduction

It is commonly believed that hadrons produced in the heavy ion collisions suffer numerous rescattering in the hot and dense matter before escaping from it, and thus can not bring out direct information about central part of the collision. That's why when one studies signatures of quark-gluon plasma (QGP), which possibly can be created in the heavy ion collisions, one usually treats hadrons as a particles, carrying information mainly about the freeze-out stage of collision. This is true if the size of the region occupied by the hot matter created in the collision is much greater than the free path length of the hadron in the hadronic gas. However, even in the collisions of the heaviest nuclei, the size of the region occupied by hot matter is of the order of the size of the colliding nuclei and comparable with free path length of hadron in hadronic gas – so hadron emission from the central region of the collision may be significant.

In this paper we consider the emission of hadrons directly from the central hot region of the collision. In particular, if QGP is created in the heavy ion collision, quarks and gluons may fly out from its pre-surface layer, transform into hadrons on its surface, and some of this hadrons can pass through surrounding hadronic gas without rescattering. Thus formed *direct* hadrons carry *direct* information about QGP surface, in contrast to usually considered 'freeze-out' hadrons originated either due to freeze-out of hadronic gas or due to decays of the resonances originated due to freeze-out of hadronic gas.

The effect of meson emission (evaporation) from the QGP surface have been discussed several times. In the paper [1] it was considered in connection with reducing of plasma pressure and thus influence on the plasma evolution. It was found that meson evaporation leads to the significant energy loss and reduction of the outward pressure on the QGP surface. Later in [2] the same estimation was performed, but hadronization of flying out quarks was described in a frame of the chromoelectric flux tube (CFT) model. It was shown that in this model the effect of meson evaporation from the plasma surface is small enough to not be important in considering of plasma evolution. It should be noted that the CFT model implies that emission takes place from the surface of a very dilute system, where the only possibility to create a meson is to born quark pair in the tube and thus discolor flying out quark. In this paper we consider a somewhat opposite situation: we suppose that dense QGP is created and the dominant mechanism of discoloring of flying out quarks or gluons is pulling into tube of soft quarks and gluons from QGP.

Hadron emission in the heavy ion collisions in the frame of quark-gluon string model was considered in [3]. It was shown that in this model final state hadrons are emitted from the whole space-time volume of the system but not from the thin freeze-out hypersurface. In our previous work we considered direct hadron emission from the static spherical volume of the QGP [4]. We showed that in this case direct hadrons strongly dominate in the soft part of the spectrum. In the present paper we consider a more realistic model which takes into account both the evolution of the hot matter and absorption by surrounding hadronic gas.

The layout of the paper is as follows: in section 2 we discuss our model in detail; in section 3 we apply our model to the S+Au collision at $200 A \cdot GeV$ (SpS) and make predictions for Pb+Pb collision at $3150 + 3150 A \cdot GeV$ (LHC); in section 4 we study the sensitivity of the results to variation of the parameters. The obtained results are summarized in the conclusion.

2 Estimation of hadronic emission from the main stages of evolution of heavy ion collision.

In our calculations we suppose that hot matter continuously emits *direct* hadrons during all stages of its evolution, from its creation until freeze-out. The direct hadrons are emitted from any elementary volume in the depth of hot hadronic gas until freeze-out takes place in this volume, and from the QGP surface until it transforms into hadronic gas. So in the collision of the heavy nuclei we have three main hadronic sources: direct hadrons from the QGP surface, direct hadrons from hadronic gas, and hadrons originated due to hadronic gas freeze-out (freeze-out hadrons). To calculate the multiplicity and p_t distribution of the direct hadrons, we evaluate quark, gluon, and hadron emission rates (i.e. the number of particles emitted from unit volume per unit time) and integrate them over the space-time volume occupied by expanding matter. Taking into account possible rescattering of the flying out direct hadrons, we use the probability to fly out:

$$P = \exp \left\{ - \int \frac{dx}{\lambda(x)} \right\}, \quad (1)$$

where integration is done over the path of the hadron in the hot hadronic gas, $\lambda(x)$ - depending on the local energy density free path length of the hadron in the hadronic gas. We use the same expression, though with different free path lengths, for the probability for quarks and gluons to fly out from the QGP and hadronize on its surface. To incorporate collective phenomena and energy-momentum conservation in order to find the space-time energy density distribution and thus estimate absorption by the hadronic gas, we use a hydrodynamic model of expansion of the hot matter. As a first step we do not consider emission of heavy mesons and resonances, but restrict ourselves to the emission of pions. Also in estimates of hydrodynamic expansion we suppose that hadronic gas consists only of pions. We describe hydrodynamic expansion of the hot matter using the refined version of Bjorken (scaling) hydrodynamics including transverse expansion. Hydrodynamic expansion stops when the energy density in the particular elementary volume becomes as low as the freeze-out one, and in the further evolution pions in this volume are treated as free particles.

Below we consider in detail the main points of our calculation: estimates of the free path lengths of the particles in the hot matter, estimates of the emission rate of the particles, description of hadronization of quarks or gluons flying out from the QGP on its surface, and description of the hydrodynamic expansion.

2.1 Quark, gluon and pion free path lengths in the medium.

Let us estimate the free path length of a quark or gluon in the quark-gluon plasma. Quark or gluon propagation in the quark-gluon plasma is described by two parameters: color and momentum relaxation free path lengths. The first is the length on which color of the quark or gluon changes due to soft gluon exchange with surrounding plasma, the second is the length on which the momentum of the particle changes significantly due to more or less hard scattering on gluons and quarks of the plasma. This two lengths are related as $\lambda_c \approx \alpha_s \lambda_m$. Our estimates depend only on the momentum relaxation free path lengths. To estimate them we use the

following expression:

$$\lambda_i^{-1}(\varepsilon_1) = \sum_j \int \frac{1}{2\varepsilon_1} \frac{d^3 p_2}{2\varepsilon_2 (2\pi)^3} f(\varepsilon_2) \frac{d^3 p_3}{2\varepsilon_3 (2\pi)^3} (1 \pm f(\varepsilon_3)) \frac{d^3 p_4}{2\varepsilon_4 (2\pi)^3} (1 \pm f(\varepsilon_4)) \quad (2)$$

$$(2\pi)^4 \delta(p_1 + p_2 - p_3 - p) |M_{ij}|^2,$$

where only two-particle reactions are taken into account, $i, j \in \{q, \bar{q}, g\}$, ε, p - energy and momentum of the initial (indexes 1,2) and final (indexes 3,4) partons, $f(\varepsilon)$ - distribution functions (Bose or Fermi), M_{ij} - matrix element of the reaction. In the case of Boltzman distributions $f(\varepsilon)$ eight integrations in (2) can be performed analytically:

$$\lambda_i(\varepsilon) = \left[\frac{1}{16\pi^3} \frac{T}{\varepsilon^2} \sum_j \int_{2m^2}^{\infty} s \sigma_{ij}(s) \ln \left(1 - \exp \left(-\frac{s}{4\varepsilon T} \right) \right) ds \right]^{-1}. \quad (3)$$

We use the following cross-sections of the reactions $qq \rightarrow qq$, $q\bar{q} \rightarrow q\bar{q}$, $qq' \rightarrow qq'$, $qg \rightarrow qg$, $q\bar{q} \rightarrow gg$, $gg \rightarrow gg$ correspondingly (q denotes quark, g - gluon, q' - quark with other than q flavor):

$$\begin{aligned} \sigma_{qq} &= \frac{4}{9} \frac{\pi\alpha_s^2}{s} \left(1 - 2\frac{m^2}{s} + 2\frac{s}{m^2} - 2\frac{s}{s-m^2} - \frac{8}{3} \ln \left(\frac{s-m^2}{m^2} \right) \right) \\ \sigma_{q\bar{q}} &= \frac{32}{27} \frac{\pi\alpha_s^2}{s} \left(1 - \frac{9}{4} \frac{m^2}{s} + \frac{3}{4} \frac{s}{m^2} - \frac{3}{4} \frac{s}{s-m^2} + \frac{3}{4} \frac{m^4}{s^2} - \frac{1}{2} \frac{m^6}{s^3} - \ln \left(\frac{s-m^2}{m^2} \right) \right) \\ \sigma_{qq'} &= \frac{4}{9} \frac{\pi\alpha_s^2}{s} \left(1 - 2\frac{m^2}{s} + 2\frac{s}{m^2} - 2\frac{s}{s-m^2} - 2 \ln \left(\frac{s-m^2}{m^2} \right) \right) \\ \sigma_{qg} &= \frac{31}{9} \frac{\pi\alpha_s^2}{s} \left(1 - 2\frac{m^2}{s} + \frac{45}{62} \frac{s}{m^2} - \frac{45}{62} \frac{s}{s-m^2} - \frac{45}{62} \ln \left(\frac{s-m^2}{m^2} \right) \right) \\ \sigma_{ann} &= \frac{67}{9} \frac{\pi\alpha_s^2}{s} \left(1 - \frac{104}{67} \frac{m^2}{s} - \frac{90}{67} \frac{m^4}{s^2} + \frac{60}{67} \frac{m^6}{s^3} + \frac{32}{67} \ln \left(\frac{s-m^2}{m^2} \right) \right) \\ \sigma_{gg} &= \frac{123}{8} \frac{\pi\alpha_s^2}{s} \left(1 - \frac{675}{328} \frac{m^2}{s} + \frac{8}{41} \frac{s}{m^2} - \frac{8}{41} \frac{s}{s-m^2} + \frac{57}{328} \frac{m^4}{s^2} - \frac{19}{164} \frac{m^6}{s^3} - \frac{57}{164} \ln \left(\frac{s-m^2}{m^2} \right) \right). \end{aligned} \quad (4)$$

To incorporate medium effects, we use screening mass $m^2 = 4\pi\alpha_s T^2$ instead of current masses of light quarks and zero mass of gluon (see e.g. [7]). Substituting cross-sections (4) into (3), and performing resting integration numerically with $\alpha_s = 0.3$, we obtain quark and gluon free path lengths in the QGP, see fig.1. In our calculations we use the following fits to these free path lengths:

$$\lambda_q = \frac{0.2}{T^{0.9}}, \quad \lambda_g = \frac{0.45}{T^{0.9}}. \quad (5)$$

where λ in fm and T in GeV . This result is consistent with estimates of the energy loss of the quark or gluon in the QGP (see e.g. [7]). Our estimates are valid if the energy of the particle is large with respect to the temperature of the plasma, but as a first step we extrapolate found free path lengths to the energies of the order of the temperature of the QGP.

To estimate pion free path length in the pionic gas we take advantage of (2) and perform all possible integrations analytically, assuming non-zero pion mass. As a result we obtain following formula:

$$\lambda_{\pi^i}(\varepsilon) = \left[\frac{1}{16\pi^3} \frac{T}{\varepsilon p} \sum_j \int_{4m^2}^{\infty} \sqrt{s(s-4m^2)} \sigma_{ij}(s) \ln \left(\frac{1 - \exp(-a_+)}{1 - \exp(-a_-)} \right) ds \right]^{-1} \quad (6)$$

where

$$a_{\pm} = \frac{(s\varepsilon - 2\varepsilon m^2 \pm p\sqrt{s^2 - 4sm^2})}{2m^2 T},$$

$\sigma_{ij}(s) - \pi^i \pi^j$ cross-section ($i, j = \{+, 0, -\}$), and m - pion mass. All necessary pion-pion cross-sections in the c.m. energy $\sqrt{s} = 0.2 - 1 \text{ GeV}$ (see fig.2) we take from [5], while for $\sqrt{s} > 1 \text{ GeV}$ we take the sum of cross-sections $\sigma_i = \sum_j \sigma_{ij}$ as constant of order 20 mb . Variation of σ_i for $\sqrt{s} > 1 \text{ GeV}$ leads to slight variations of the slope in the dependence of free path length on the energy of the pion. Estimations of the pionic free path length at three different temperatures of pionic gas are shown in fig.3.

2.2 Estimations of the quark, gluon and pion emission rates

In this subsection we estimate emission rates of the quark and gluon from quark-gluon plasma and pions from pionic gas. In this calculation we assume that the particle is emitted at the moment of its last scattering on other one or at the moment when the particle is born. Thus we do not take into account a few particles which born before we begin consideration of the evolution of the system and pass through the system without rescattering.

In our estimates of quark and gluon emission rate we take into account only two-particle reactions like $qq \rightarrow qq$, $q\bar{q} \rightarrow q\bar{q}$, $qq' \rightarrow qq'$, $qg \rightarrow qg$, $q\bar{q} \rightarrow gg$, $gg \rightarrow gg$ - the same as those, taken for the free path lengths evaluation. Thus the emission rate of the parton i from quark-gluon plasma can be written as

$$\varepsilon \frac{d^7 R_i}{d^3 p d^4 x} = \sum_j \int \frac{d^3 p_1}{2\varepsilon_1 (2\pi)^3} f(\varepsilon_1) \frac{d^3 p_2}{2\varepsilon_2 (2\pi)^3} f(\varepsilon_2) \frac{d^3 p_3}{2\varepsilon_3 (2\pi)^3} (1 \pm f(\varepsilon_3)) \times (1 \pm f(\varepsilon)) \frac{(2\pi)^4 \delta(p_1 + p_2 - p_3 - p)}{2(2\pi)^3} |M_{ij}|^2, \quad (7)$$

where the sum is over all possible two-particle reactions, p_1, p_2 - momentum of the initial particles, p_3, p - momentum of the final particles, $f(\varepsilon)$ - Fermi or Bose distributions for quarks and gluons respectively, $(1 \pm f(\varepsilon))$ - Fermi blocking or Bose enhancement for final state quarks and gluons respectively, and M_{ij} - matrix element for the process of the i on j scattering.

This formula is in agreement with estimates of quark and gluon emission from the unit of surface per unit of time of semi-infinite QGP with constant temperature. On one hand this is just thermal black body radiation and described by the formula:

$$\varepsilon \frac{d^6 R^{thermo}}{d^3 p d^2 S dt} = \frac{d \cdot \varepsilon}{(\exp(\varepsilon/T) \pm 1)}$$

where d - degeneracy ($d = 16$ for gluons, $d = 24$ for u, d quarks). On the other hand we can evaluate the same quantity from the microscopic approach - via emission rate and momentum relaxation free path length:

$$\varepsilon \frac{d^6 R_i^{micro}}{d^3 p d^2 S dt} = 2\pi \int dx \int \sin(\theta) d\theta \exp\left(-\frac{x}{\lambda(\varepsilon) \cdot \cos(\theta)}\right) \cdot \varepsilon \frac{d^7 R_i}{d^3 p d^4 x}. \quad (8)$$

Equation (8) relates emission rate with free path length as:

$$\varepsilon \frac{d^7 R_i}{d^3 p d^4 x} = \frac{d_i}{\lambda_i(\varepsilon)} \frac{\varepsilon}{(\exp(\varepsilon/T) \pm 1)}. \quad (9)$$

In our calculations we use (9) instead of separate evaluation of free path length and emission rate.

To take into account the collective velocity of the emitting volume, we use the invariance of $\varepsilon d^3 R / d^3 p$ with respect to Lorentz boosts. So the right side of the (7) is invariant too. In the rest frame of the volume we have $\varepsilon d^3 R / d^3 p = f(\varepsilon)$, then in the laboratory frame, where volume moves with 4-velocity u , we have $\varepsilon d^3 R / d^3 p = f(p \cdot u)$, where p is 4-momentum of the particle.

2.3 Hadronization of the quarks and gluons on the plasma surface.

To describe hadronization of a quark or gluon crossing the QGP surface, we assume that the flying out parton deforms the plasma surface by creation of a string-like tube, which breaks if the colorless state is formed in the tube and one final hadron is born. The energy of the final hadron is in the range $m_h < \varepsilon < \varepsilon_p$ with constant probability for each value. So p_t distribution of the partons $d^3 R^{part} / dy d^2 p_t$, determines p_t distribution of the final hadrons:

$$\frac{d^3 R^{hadr}}{dy d^2 p_t} = \frac{1}{\varepsilon} \int_{\varepsilon}^{\infty} d\omega \cdot \frac{d^3 R^{part}}{dy d^2 p_t}, \quad (10)$$

where it is assumed that one flying out parton transforms into one final hadron. It can be easily seen that this formula describes the decay of the particle given only one restriction: the energy of the initial particle must be greater than energy of the final one. In this paper we take into account decays into pions only, inclusion of the resonances is in progress.

We stress that the hadronization of the quark or gluon in this process differs from hadronization in the e^+e^- annihilation. If QGP is formed then a quark or gluon flying out from its surface may 'pull' soft quarks and gluons from the plasma into the string. As a result of this discoloring the string is broken and final state hadron is formed. In the e^+e^- annihilation the only possibility to create a final hadron is to born $q\bar{q}$ pair in the string. So the physics of these two processes is different and applicability of the string model as it is used in the description of e^+e^- annihilation to the description of the quark and gluon hadronization on the QGP surface is questionable.

A few words should be added about formation of the direct pions emitted from QGP. The pion is a rather extensive and complicated object, and it takes some time to form its structure from the piece of the string flying out from QGP. This formation of the structure takes at least the time needed for light to cross the pion, i.e. approximately $0.6 fm/c$ in the rest frame. During this formation time the pion does not interact with surrounding hadronic gas as a real pion, but rather as a pair of quarks. Corresponding quark-quark cross-sections $\sigma_{qq} \sim 2 - 10 mb$ are approximately 10 times smaller than $\sigma_{\pi\pi} \sim 20 - 130 mb$, and in our calculations we accept that during formation time of order $\tau_0 = 0.6 fm/c$ in the rest frame after emission from the plasma surface the emitted pion does not interact with hadronic gas.

2.4 Hydrodynamic description of the evolution.

In order to take into account absorption of the direct hadrons in hot expanding hadronic gas surrounding QGP and estimate time of life of the QGP we use a hydrodynamic approach. This is just an expression of local energy and momentum conservation:

$$\partial_\mu T^{\mu\nu} = 0, \quad (11)$$

where $T^{\mu\nu}$ is the energy-momentum tensor:

$$T^{\mu\nu}(x) = (\varepsilon(x) + p(x)) \cdot u^\mu u^\nu - g^{\mu\nu} \cdot p(x). \quad (12)$$

Here $\varepsilon(x)$ and $p(x)$ – local energy density and pressure respectively, u^μ – four-velocity of the medium and $g^{\mu\nu}$ metric tensor ($g = \text{diag}(1, -1, -1, -1)$). Having in mind applications of our approach to predictions for LHC energy, we introduce some simplifications into initial conditions and equations suitable for high energy case: we suppose that Bjorken (scaling) hydrodynamics [12] is applicable. Simplifications, proposed by Bjorken, are based on the fact that in midrapidity interval all quantities are independent of rapidity. So hydrodynamic equations must be invariant with respect to the Lorenz boosts along collision axis. That is four-velocity can be parametrized in the form

$$u^\mu = \gamma \left(\frac{t}{\tau}, \vec{v}, \frac{z}{\tau} \right),$$

where $\tau = \sqrt{t^2 - z^2}$, $\gamma = (1 - v^2)^{-\frac{1}{2}}$, v – transverse velocity. With these assumptions the hydrodynamic equations in the midrapidity region ($z = 0$) can be rewritten as

$$\begin{aligned} \partial_\tau (\gamma^2 w(r, \tau)) + \partial_r (\gamma^2 v w(r, \tau)) + \gamma^2 w(r, \tau) \tau^{-1} + \gamma^2 v w(r, \tau) r^{-1} - \partial_\tau p(r, \tau) &= 0 \\ \partial_\tau (\gamma^2 v w(r, \tau)) + \partial_r (\gamma^2 v^2 w(r, \tau)) + \gamma^2 v w(r, \tau) \tau^{-1} + \gamma^2 v^2 w(r, \tau) r^{-1} + \partial_r p(r, \tau) &= 0, \end{aligned} \quad (13)$$

where $w(r, \tau) = \varepsilon(r, \tau) + p(r, \tau)$ – entalpy density.

We solve equation (13) numerically using the MacCormack technique. This is explicit predictor-corrector Euler algorithm, which allows second order accuracy on a spatial and time grid step. To rewrite (13) in terms of final differences it is convenient to introduce the following variables:

$$U = \begin{pmatrix} \gamma^2 w - p \\ \gamma^2 v w \end{pmatrix}; \quad F = \begin{pmatrix} \gamma^2 v w \\ \gamma^2 v^2 w + p \end{pmatrix}; \quad H = \begin{pmatrix} \gamma^2 w (\tau^{-1} + v r^{-1}) \\ \gamma^2 v w (\tau^{-1} + v r^{-1}) \end{pmatrix}$$

In these variables equation (13) can be rewritten in a discrete form (subscript correspond to the spatial sell number, superscript correspond to the time level):

$$\begin{aligned} \bar{U}_i^j &= U_i^j - \Delta\tau \left((F_{i+1}^j - F_i^j) / \Delta r + H_i^j \right) + D_i^j \\ U_i^{j+1} &= \frac{1}{2} \left[(U_i^j + \bar{U}_i^j) - \Delta\tau \left((\bar{F}_i^j - \bar{F}_{i-1}^j) / \Delta r + \bar{H}_i^j \right) \right] + \bar{D}_i^j \end{aligned} \quad (14)$$

where $\bar{F}_i^j, \bar{H}_i^j, \bar{D}_i^j$ are evaluated using \bar{w}_i^j, \bar{v}_i^j taken from \bar{U}_i^j , and D_i^j – term, corresponding to the smoothing, proposed by Zmakin and Fursenko [13]. This term conserves global energy and momentum and allows working with various hydrodynamic disturbances such as shock waves and first order phase transition. It can be written as

$$D_i^j = \begin{cases} \varphi_i^j, & (\varphi_{i-1}^j \cdot \varphi_{i-2}^j < 0) \cup (\varphi_i^j \cdot \varphi_{i-1}^j < 0) \\ 0, & (\varphi_{i-1}^j \cdot \varphi_{i-2}^j > 0) \cap (\varphi_i^j \cdot \varphi_{i-1}^j > 0) \end{cases} \quad (15)$$

where $\varphi_i^j = Q \cdot (U_{i+1}^j - U_i^j)$, and Q – parameter of smoothing (the best results are obtained with $Q \approx 0.1 - 0.15$).

Hydrodynamic equations must be accomplished by equations of state. In our calculations we used the simplest one, including first order phase transition at the temperature T_c and freeze-out of the pionic gas at the temperature T_{freeze} :

$$P(\varepsilon) = \begin{cases} \frac{\varepsilon}{3} - \frac{4}{3}B, & \varepsilon \geq \varepsilon_{qgp} \\ P_0, & \varepsilon_{qgp} \geq \varepsilon \geq \varepsilon_{had} \\ \frac{\varepsilon}{3}, & \varepsilon_{had} \geq \varepsilon \geq \varepsilon_{freeze} \\ 0, & \varepsilon_{freeze} \geq \varepsilon \end{cases} \quad (16)$$

where B – energy density of perturbative vacuum of QCD (bag constant), ε_{qgp} – energy density of the QGP before phase transition, ε_{had} – energy density of the pionic gas after phase transition and ε_{freeze} – energy density of the pionic gas at freeze-out:

$$\varepsilon_{qgp} = d_{qgp} \frac{\pi^2}{30} T_c^3 + B, \quad \varepsilon_{had} = d_{had} \frac{\pi^2}{30} T_c^3, \quad \varepsilon_{freeze} = d_{had} \frac{\pi^2}{30} T_{freeze}^3$$

where $d_{qgp} = 37$ – degeneracy of the QGP, $d_{had} = 3$ – degeneracy of the pionic gas.

It is well known that the hydrodynamic description assumes local thermal equilibrium, which surely can not be reached in the very beginning of the collision when the colliding nuclei penetrate each other. So to properly describe a collision we have to either describe the pre-equilibrium dynamics (i.g. three-fluid hydrodynamics [14]) or introduce some parameters such as initial time (initial volume) and initial spatial energy density and velocity distributions. In this paper we use the latter approach: we introduce these parameters into the scheme and adjust them to reproduce measured pion multiplicity and p_t spectrum. In our estimates we use an initial spatial energy density distribution proportional to the integral of the nuclear energy density along the beam axis:

$$\varepsilon_{in}(r) = \varepsilon_0 \int_{-\infty}^{\infty} \left[1 + \exp \left(\frac{(\sqrt{r^2 + l^2} - R_{in})}{w} \right) \right]^{-1} dl, \quad (17)$$

where $\varepsilon_0 = d_{qgp} \frac{\pi^2}{30} T_{in}^3 + B$ if we assume QGP formation, and $\varepsilon_0 = d_{had} \frac{\pi^2}{30} T_{in}^3$ in the case of pure hadronic gas. R_{in} and w are taken from known nuclear density distribution, e.g. for nuclei S^{32} we have $R_{in} = 3.5 \text{ fm}$, $w = 0.65 \text{ fm}$. For initial radial velocity distribution, we take $v_{in}(r) = 0$.

3 Obtained results.

3.1 Predictions for S+Au collision at 200 $A \cdot \text{GeV}$.

Now let us apply our model to the S+Au collisions at 200 $A \cdot \text{GeV}$, which were studied experimentally. We consider two possible cases of evolution: with and without QGP creation. In both cases we adjust the free parameters of the model to reproduce measured ([15]) pion multiplicity and p_t distribution at midrapidity. In the case of QGP creation, the experimental data are better described by the following set of parameters:

$$T_{in} = 180 \text{ MeV}, \quad \tau_{in} = 1.3 \text{ fm}/c, \quad R_{in} = 3.5 \text{ fm}, \quad T_c = 150 \text{ MeV}, \quad T_{freeze} = 140 \text{ MeV}.$$

In the case of pure hadronic gas the better description is obtained with another set:

$$T_{in} = 180 \text{ MeV}, \tau_{in} = 4.3 \text{ fm}/c, R_{in} = 7 \text{ fm}, T_{freeze} = 140 \text{ MeV}.$$

Estimation of p_t distributions of π^0 at midrapidity ($y \approx 3$) for the different pionic sources in this reaction with assumption of QGP creation is shown in fig.4. The dotted line corresponds to the direct pions from QGP surface, the dashed line corresponds to the direct pions from the depth of pionic gas and the solid line corresponds to the freeze-out pions. Direct pions from QGP surface dominate in the p_t range $0 - 0.5 \text{ GeV}/c$ while at large p_t freeze-out pions dominate.

Naively one could expect the inverse situation: emissions from the hotter phase dominate in the hard part of the spectrum while emissions from the cooler phase dominate in the soft one. However, if we take into account the collective velocity of pionic gas in hydrodynamic expansion, we find that the effective temperature of the spectrum of freeze-out pions $T' = T\sqrt{(1+u)/(1-u)}$ (u - collective velocity of the volume, T - temperature of pionic gas in the rest frame) for reasonable collective velocities $u > 0.3$ is larger than even initial temperature. Anywhere, direct pions strongly contribute to total multiplicity: at midrapidity multiplicity of the direct pions is $dN^{dir}/dy = 70$ while multiplicity of freeze-out ones is $dN^{freeze}/dy = 50$. So even for collisions of not too heavy nuclei at relatively low energies, when QGP (if created) lives a rather short time, direct pion contribution to total pionic yield is significant.

If we do not assume QGP creation, and consider evolution of pure pionic gas, we obtain p_t distributions of π^0 at midrapidity ($y \approx 3$), shown in fig. 5. Dashed line corresponds to the direct pions from pionic gas, solid line corresponds to the freeze-out pions. In this case of evolution direct pions do not dominate anywhere and the main contribution comes from freeze-out pions: multiplicity at midrapidity of the direct pions is $dN^{dir}/dy = 8$ while this value for freeze-out pions is $dN^{freeze}/dy = 110$.

The comparison of total p_t distributions of π^0 at midrapidity, calculated assuming two possible cases of evolution with experimental data is shown in fig.6. The dotted line corresponds to the estimate assuming QGP formation, the solid line corresponds to the estimate considering pure pionic gas evolution. Circles correspond to p_t distribution of π^0 , obtained by WA80 collaboration for S+Au at $200 \text{ A} \cdot \text{GeV}$ [15]. The results of this calculation, assuming pure pionic gas evolution, better describe experimental results, except a region at small p_t . This exceeding of the experimental distribution can be explained by decays of resonances (N, Δ , etc.). In the case of QGP creation it is impossible to describe p_t distribution as well as in the case of pure pionic gas, as long as we use reasonable values for parameters of the model.

Direct pions may carry out a significant part of the energy from the central hot region of the collision and thus strongly affect the evolution of the system. To compare evolution of the hot matter in the S+Au collision at $200 \text{ A} \cdot \text{GeV}$ with direct pion production and without it, we plot contour curves for constant energy density for these two cases – see fig.7. The left plot corresponds to the evolution with direct pion emission, the right plot corresponds to the evolution without direct pion emission. Initially the system is in the QGP state (black region), then it transforms into mixed phase, expands longitudinally and transversely and thus cools, until pure pionic gas is formed (gray region). We see that if we take into account direct pion emission, then time of life decreases approximately 1.3 times in comparison to the case of evolution without direct pion emission. Contour curves for constant velocity from 0.1 with step 0.1 for this two cases are shown in fig.8. Our calculation stops when all pionic gas freezes-out,

so in fig. 8 contour curves are shown only for $t < 12 \text{ fm}/c$ for the first case and for $t < 15 \text{ fm}/c$ for the second case. If we compare fig.7 and fig.8, we see that matter is accelerated mainly during expansion of pionic gas, mixed phase as a phase with $dP/dr = 0$, where P - pressure, does not contribute into this acceleration. In the first case the velocity obtained by pionic gas is lower than the one obtained in the second case – because of longer life time and thus longer acceleration.

Therefore if QGP is formed in this collision, direct pions are abundantly emitted from its surface and strongly contribute to the total pionic multiplicity. Direct pions carry out a significant part of the energy from the central part of the collision and thus decrease life time of the system.

3.2 Prediction for Pb+Pb collision at $3150 + 3150 \text{ A} \cdot \text{GeV}$.

In the Pb+Pb collisions at LHC energy space-time volume occupied by QGP is expected to be much larger than one at the SpS energies, and thus direct pion emission is expected to be much more intense. In this section we estimate contribution of the direct pions to the total pionic yield in Pb+Pb collision at LHC energy. We use the following initial conditions, corresponding to total multiplicity $dN/dy \sim 4000$, predicted by Monte-Carlo event generators:

$$T_{in} = 350 \text{ MeV}, \tau_{in} = 1 \text{ fm}/c, R_{in} = 6.5 \text{ fm},$$

and transitions and freeze-out temperatures, used in description of S+Au data:

$$T_c = 150 \text{ MeV}, T_{freeze} = 140 \text{ MeV}.$$

The result of this evaluation is shown in fig.9. The dotted line corresponds to the direct pions from QGP surface, the dashed line corresponds to the direct pions from pionic gas and the solid line corresponds to the freeze-out pions. Direct pions from QGP surface dominate up to an order of magnitude in the soft part of the distribution $p_t < 0.7 \text{ GeV}$ while freeze-out pions dominate in the hard part. Direct pions from pionic gas do not dominate anywhere. We find that multiplicities per unit rapidity at $y \approx 0$ of direct and freeze-out pions are $dN^{dir}/dy = 3000$, $dN^{freeze}/dy = 1200$ respectively.

Comparison of space-time evolutions of the hot matter created in the collision with and without direct pion emission can be made using contour curves of constant energy density shown in fig.10. The black region corresponds to the pure QGP phase, the white region corresponds to the mixed phase and the gray region corresponds to the pure pionic gas. If we do not take into account direct pion emission, then the collective flow becomes more significant (bumps on the contour curves on the right plot), otherwise cooling takes place mainly due to direct pion emission (smoother curves on the left plot).

Thus the direct pions are abundantly emitted by surface of QGP if it is created in the Pb+Pb collision at LHC energy, such that $\sim 70\%$ of pions produced in this collision are direct pions flying out from the QGP surface without further rescattering in surrounding pionic gas and carrying out direct information about QGP. Also the direct pions carry out a significant part of energy and influence the evolution of the system: the system cools more due to direct pion emission rather than hydrodynamic expansion.

4 Stability to variation of parameters.

We see that direct pions emitted from QGP surface dominate at small p_t at SpS and LHC energies. This effect is not large enough to be ensured that it will not disappear for any reasonable choice of the model parameters. Indeed, we use several parameters (such as freeze-out temperature T_{freeze} , phase transition temperature T_c , quark, gluon, and pion free path lengths, initial energy density and velocity distributions, initial time) which can not be evaluated exactly; instead, we obtain their value from more or less reliable estimates and find a relatively wide range of their possible values. So in this section we explore sensitivity of our results to variations of values of the parameters in reasonable limits.

The freeze-out temperature T_{freeze} can be varied in the range 100–140 MeV . Varying T_{freeze} we also have to vary initial temperature T_{in} to reproduce experimental p_t distribution. Results of corresponding estimates (assuming QGP creation) are shown in fig.11. Lines marked by stars correspond to $T_{in} = 150 MeV, T_{freeze} = 100 MeV$ and lines marked by circles correspond to $T_{in} = 180 MeV, T_{freeze} = 150 MeV$. Here, and until the end of the section, dotted, dashed, and solid lines correspond respectively to pions emitted directly from QGP, pions from pionic gas, and freeze-out pions. We see that the distribution of direct pions from QGP remains unaffected, the yield of direct pions from pionic gas slightly increases and p_t the distribution of freeze-out pions becomes harder. Anyway direct pions from QGP dominate at soft p_t for all tested T_{freeze} .

Next, consider the transition temperature T_c (and related to it bag constant B and external pressure on QGP). Results of estimates using two different values of T_c are shown in fig.12. Lines marked by stars correspond to $T_c = 150 MeV$, lines marked by circles correspond to $T_c = 180 MeV$. Increasing T_c leads to decreasing the life time of the system (especially of the pure QGP and mixed phase) and thus to decreasing the multiplicity of direct pions from QGP. The longer evolution of the pure pionic gas (larger difference $T_c - T_{freeze}$) leads to increasing the multiplicity of direct pions from pionic gas and a slight increasing of the slope of freeze-out pions due to larger collective velocity.

A sensitivity of our results to variation of the quark and gluon free path lengths in QGP is shown in fig.13. Lines marked by circles correspond to evaluation using the values calculated in section 2.1 for quark and gluon free path lengths (5). Lines marked by stars correspond to evaluation with free path lengths twice larger then (5). We see that in the case of larger free path length, and thus lower emission rate of quarks and gluons (see (9)), the multiplicity of direct pions from QGP decreases, and (as a result of energy conservation) the multiplicity of direct pions from pionic gas and freeze-out pions increases.

To complete investigation of sensitivity of our results to the choosing of set of parameters, let us vary the free path length of pion in the pion gas (λ_π). Results of calculations using two pion free path lengths: estimated in section 2.1 (lines marked by circles) and twice larger (lines marked by stars), are shown in fig.14. Distribution of direct pions from QGP does not change significantly, so we can conclude that the depth of surrounding pionic gas is not large and absorption is low. In accordance with (9) emission rate of pions from pionic gas decreases with increasing of λ_π and thus the multiplicity of direct pions from pionic gas decreases as well.

So the domination of direct pions in the soft region is not an effect of the accidental choice of a set of parameters of the model, but a real effect, stable with respect to variation of the parameters.

5 Conclusions

We considered effect of emission of direct hadrons from the central region of the central heavy ion collision: emission of quarks and gluons from depth of QGP, their hadronization on its surface and partial flying out through surrounding hadronic gas. As a first step we estimate only emission of pions.

Estimates performed for S+Au collision at $200 A \cdot GeV$ show that if QGP is created then direct pions from the QGP surface dominate in the soft region $p_t < 0.5 GeV/c$.

In the case of pure pionic gas we find that direct pions from the depth of the gas do not dominate anywhere.

Estimation performed for Pb+Pb collision at LHC energy ($dN/dy = 4200$) shows that direct pion emission becomes more important at this energy level. We find that multiplicity of direct pions $dN^{dir}/dy = 3000$ while multiplicity of freeze-out pions $dN^{freeze}/dy = 1200$ – i.e. approximately 70% of final pions come from the QGP surface.

The direct pion emission decreases lifetime of the S+Au system at $200 A \cdot GeV$ and Pb+Pb at $3150 + 3150 A \cdot GeV$ approximately by 1.3 times.

This result is stable with respect to variation of the model parameters in a wide reasonable range.

References

- [1] M. Danos, J.Rafelski, Phys. Rev. **D 27** (1983) 671.
- [2] B. Banerjee, N. K. Glendenning, T. Matsui, Phys. Let. **127B** (1983) 453.
- [3] L.V. Bravina et al., Phys. Let. **B 354** (1995), 196.
- [4] D. Yu. Peressounko, Yu. E. Pokrovsky, T. V. Mukhanova, Phys. of Atomic Nuclei, **58**, (1995) 1450.
- [5] O. O. Patarakin, V. N. Tikhonov, private communications, the basis of the analysis can be found in O. O. Patarakin et al., Nucl. Phys. **A 598** (1996) 335.
- [6] J. L. Goity, H. Leutwyler, Phys. Let. **B 28** (1989), 517.
- [7] Xin-Nian Wang, Miclos Gyulassy, Michael Plümer, Phys. Rev. **D 51** (1995), 3436.
- [8] J. Kapusta, P. Lichard, D. Seibert, Phys. Rev. **D 44** (1991), 2774.
- [9] Li Xiong, E. Shuryak, G. E. Brown, Phys. Rev. **D 46** (1992) 3798.
- [10] K. Haglin, Phys. Rev. **C 50** (1994) 1688.
- [11] L. D. Landau, Izv. Acad. Nauk XVII Ser. Phys. (1953), 51.
- [12] J. D. Bjorken, Phys. Rev. **D 27** (1983), 140.
- [13] Zmakin, Fursenko, Sov. Journal Vych. Math. and Math. Phys. v.20,4,p.1021.

- [14] L. P. Csernai et al., Phys. Rev. **C26** (1982) 149.
- [15] R. Albrecht et al., Phys. Lett. **B 361** (1995), 14.

Figure caption

Fig.1. Free path length of a quark (q) and gluon (g) in the QGP for two temperatures of QGP and fit to them, used in our analysis.

Fig.2. Pion-pion cross-sections for c.m. energy $\sqrt{s} < 1 \text{ GeV}$ [5].

Fig.3. Free path length of a pion in pionic gas for three different temperatures of the pionic gas.

Fig.4. Differential multiplicity of direct π^0 from QGP (dotted line), direct π^0 from pionic gas (dashed line) and freeze-out π^0 (solid line) in the S+Au collision at $200 \text{ A} \cdot \text{GeV}$ in the case of QGP creation.

Fig.5. The same as fig.4, but for the case of pure pionic gas.

Fig.6. Total differential multiplicities of π^0 for S+Au collision at midrapidity ($y \approx 3$) for S+Au collision at $200 \text{ A} \cdot \text{GeV}$. Circles – distribution measured by WA80 collaboration, dotted line – result of estimate with QGP creation, solid line – result of estimate with pure pionic gas evolution.

Fig.7. Constant energy density contour curves for S+Au collision at $200 \text{ A} \cdot \text{GeV}$ for two kinds of evolutions: with and without direct pion emission. The black region corresponds to the pure QGP phase, the grey region to the pure pionic gas phase.

Fig.8. Constant velocity contour curves from 0.1 with step 0.1 for S+Au collision at $200 \text{ A} \cdot \text{GeV}$ for two kinds of evolutions: with and without direct pion emission.

Fig.9. The same as fig.4, but for Pb+Pb collision at LHC energy.

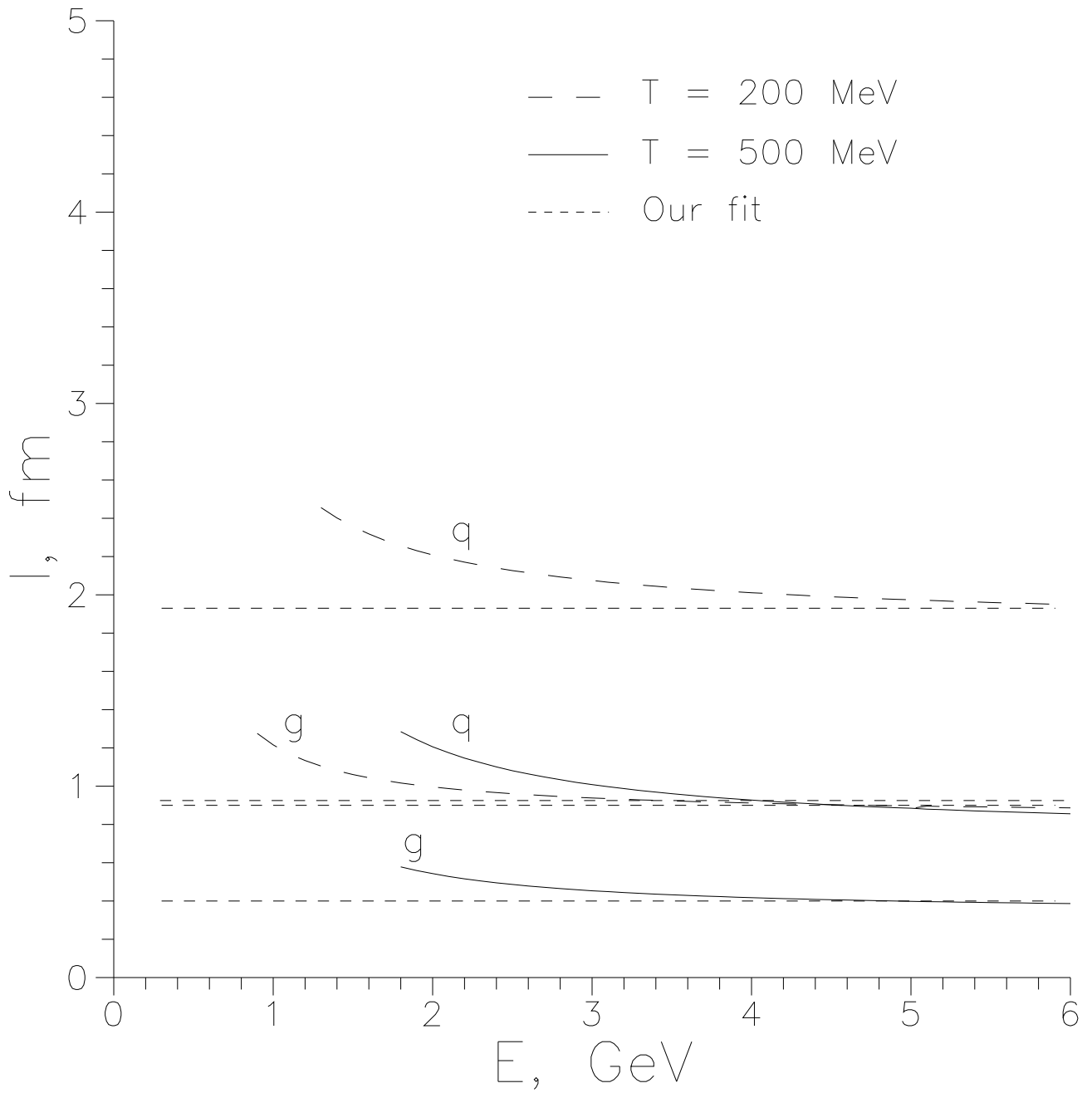
Fig.10. The same as fig.7, but for Pb+Pb collision at LHC energy.

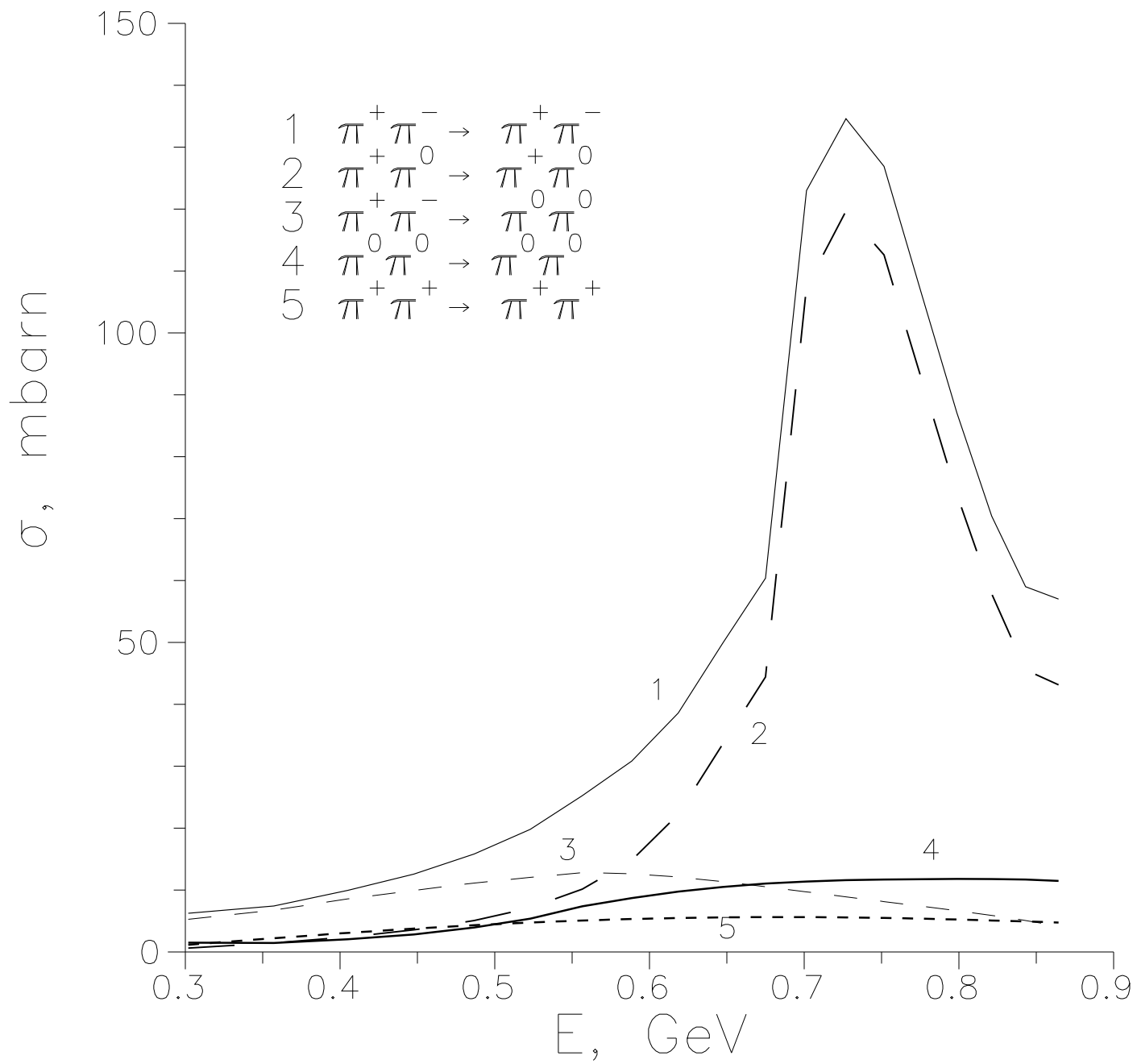
Fig.11. Sensitivity of predictions to variation of freeze-out (T_{freeze}) and initial (T_{in}) temperatures.

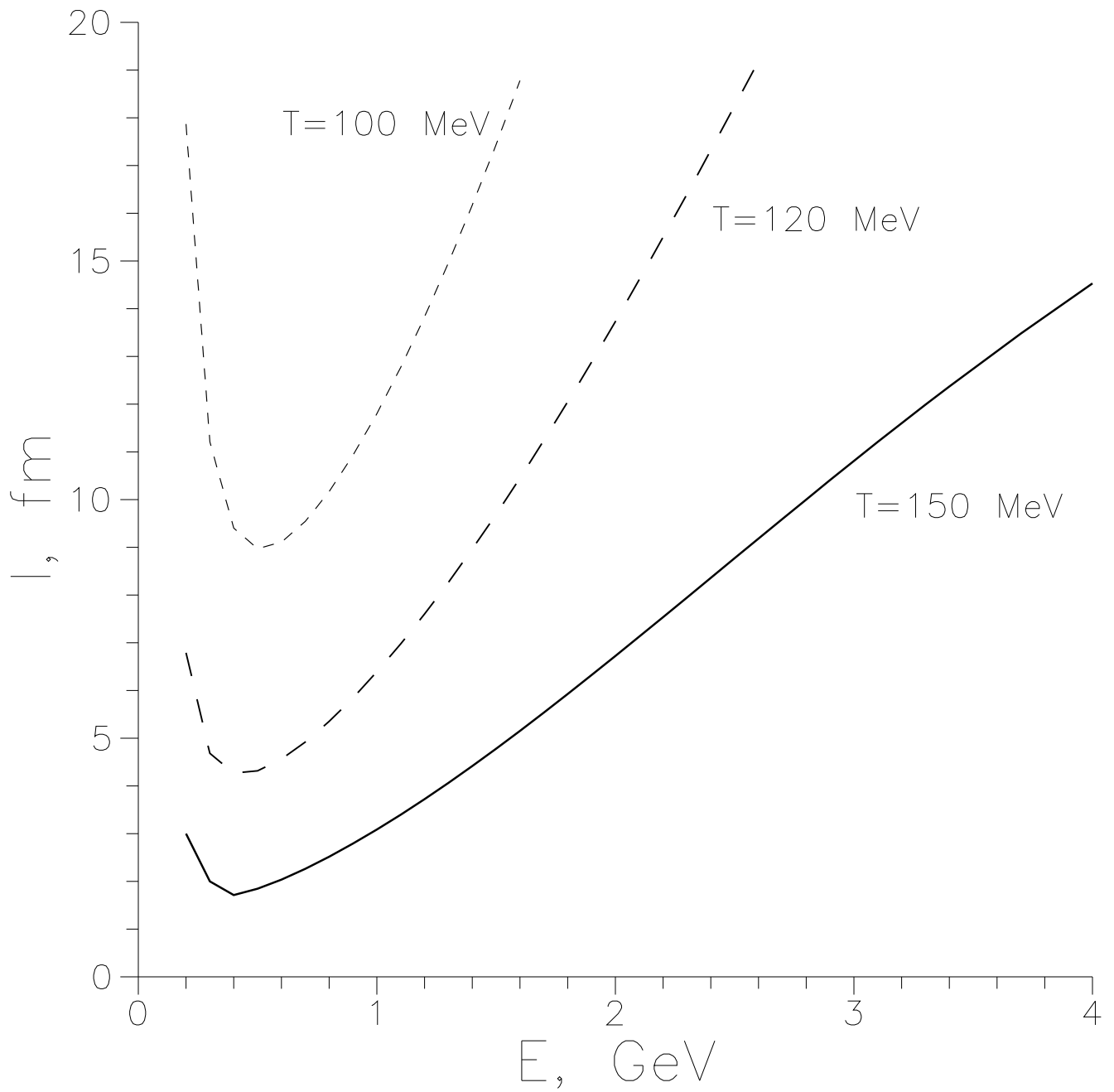
Fig.12. Sensitivity of predictions to variation of transition (T_c) temperature.

Fig.13. Sensitivity of predictions to variation of free path lengths of quarks (λ_q) and gluons (λ_g) in QGP.

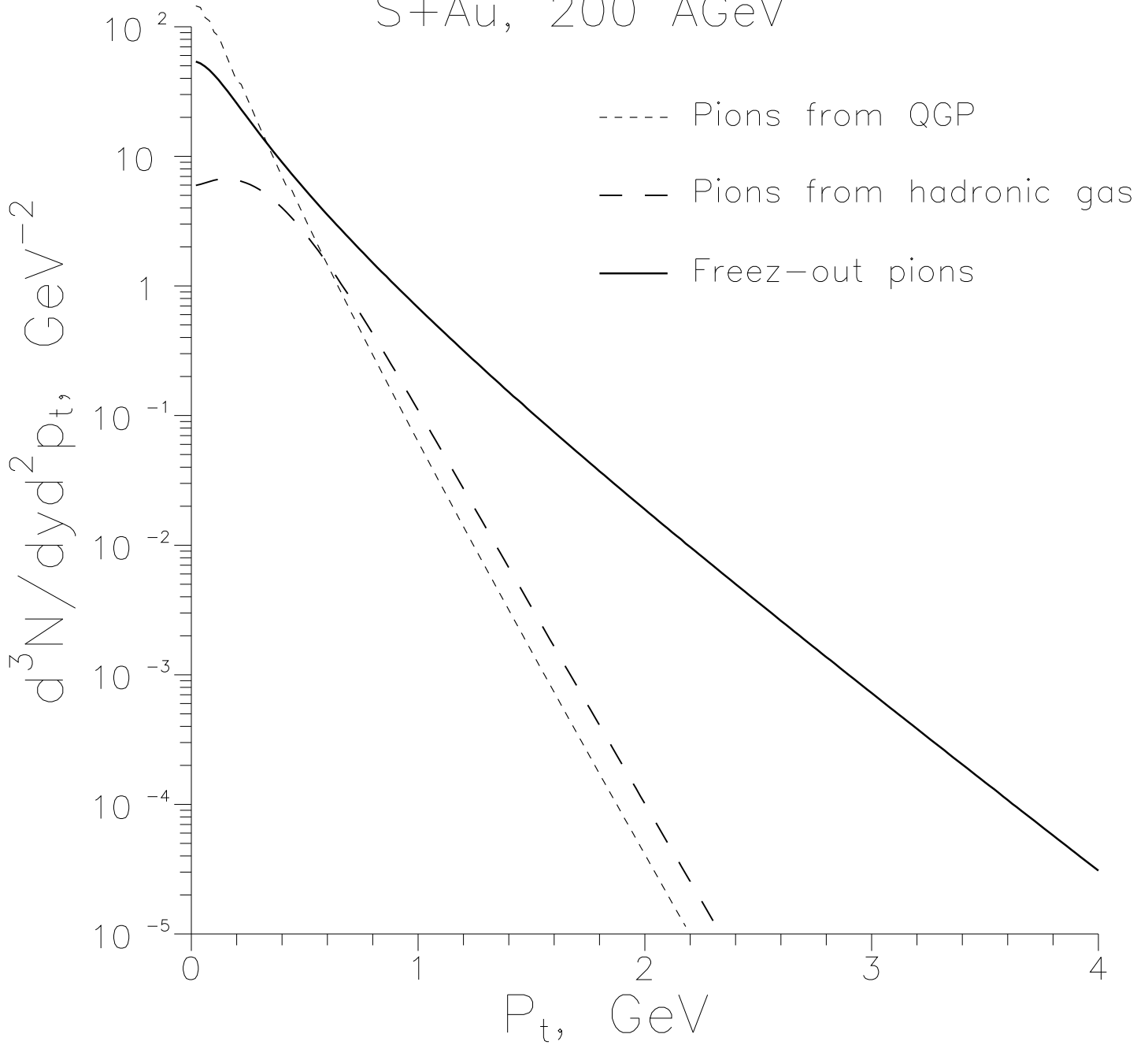
Fig.14. Sensitivity of predictions to variation of free path length of pions in the pionic gas (λ_π).

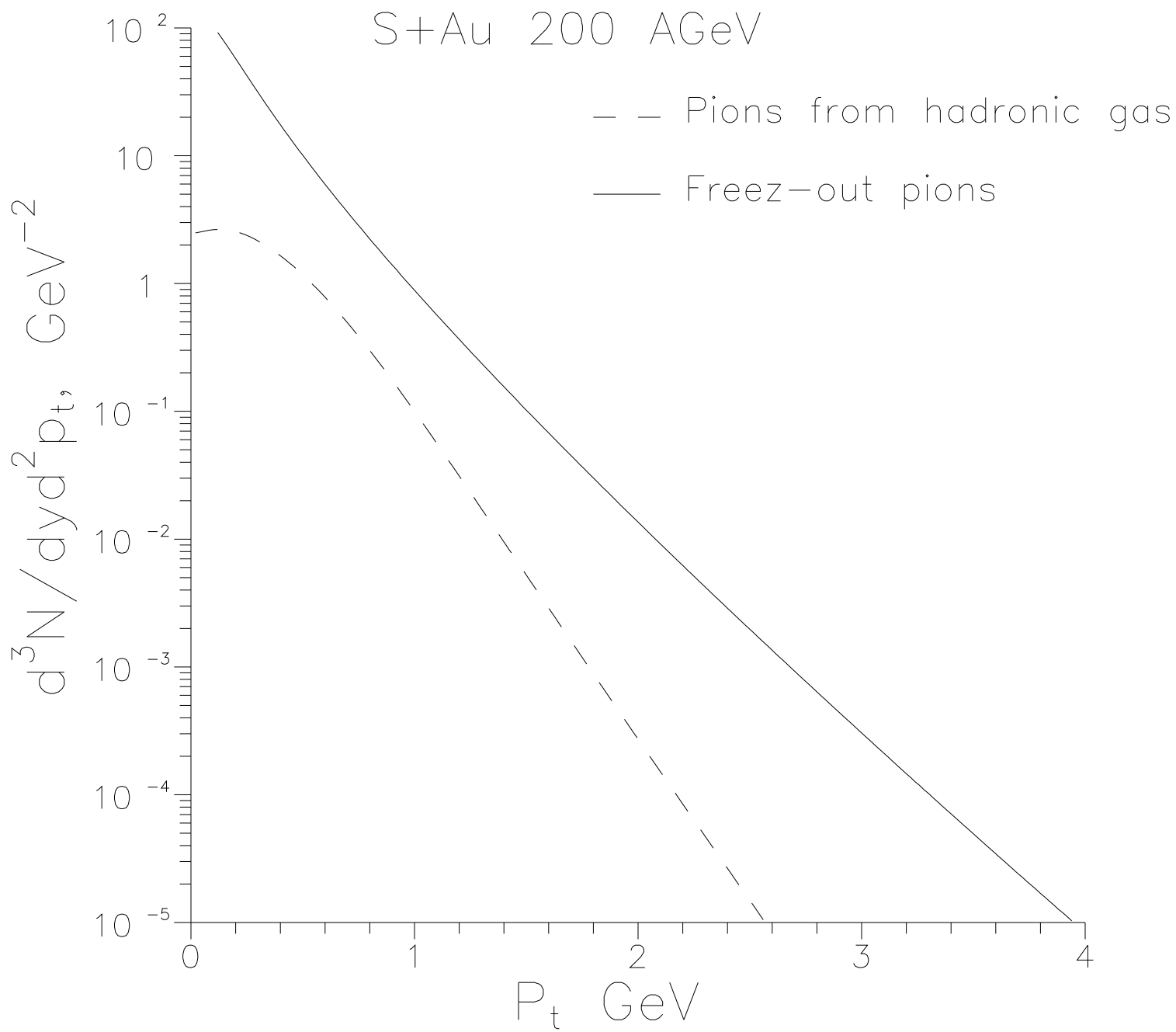


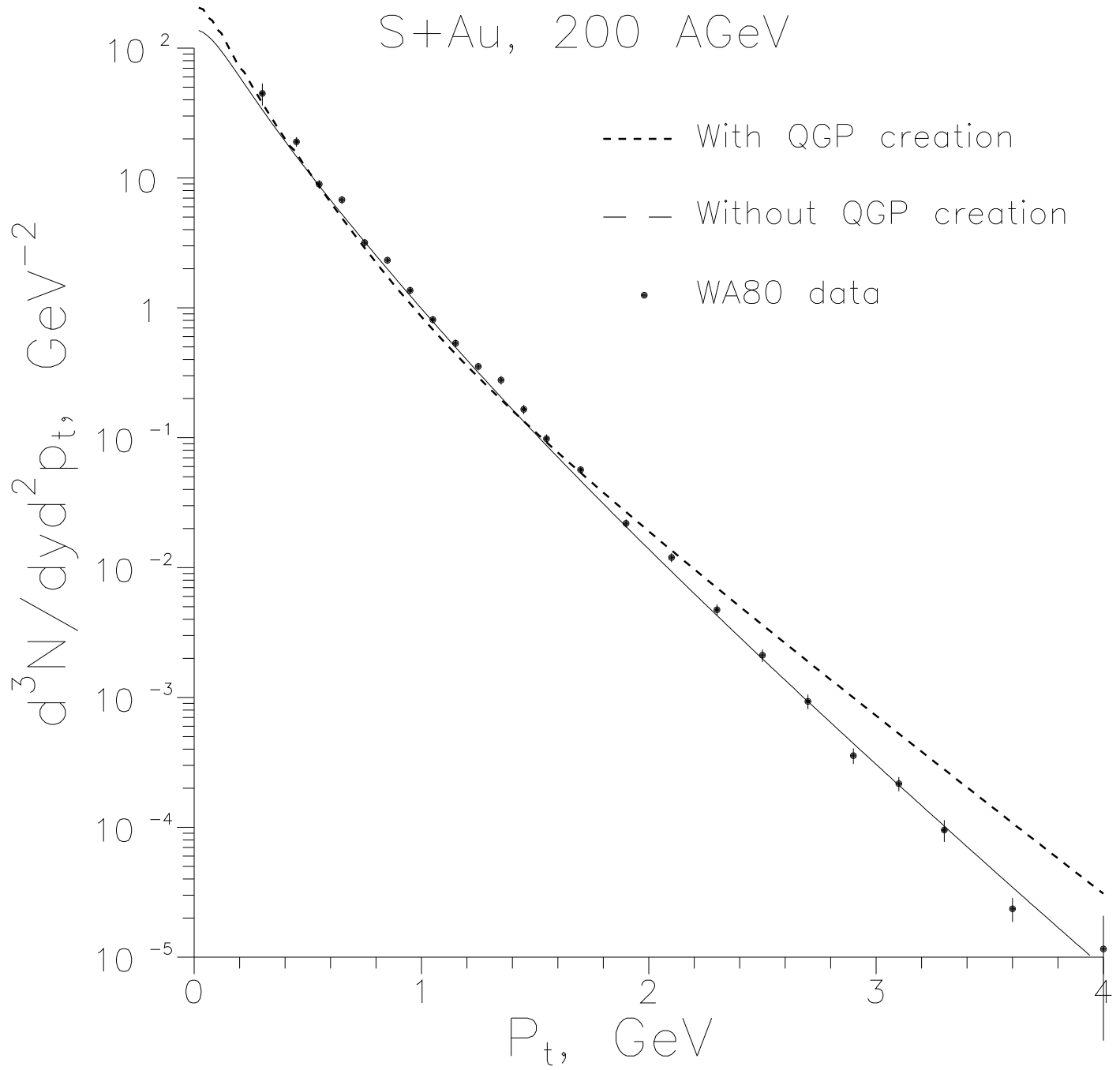


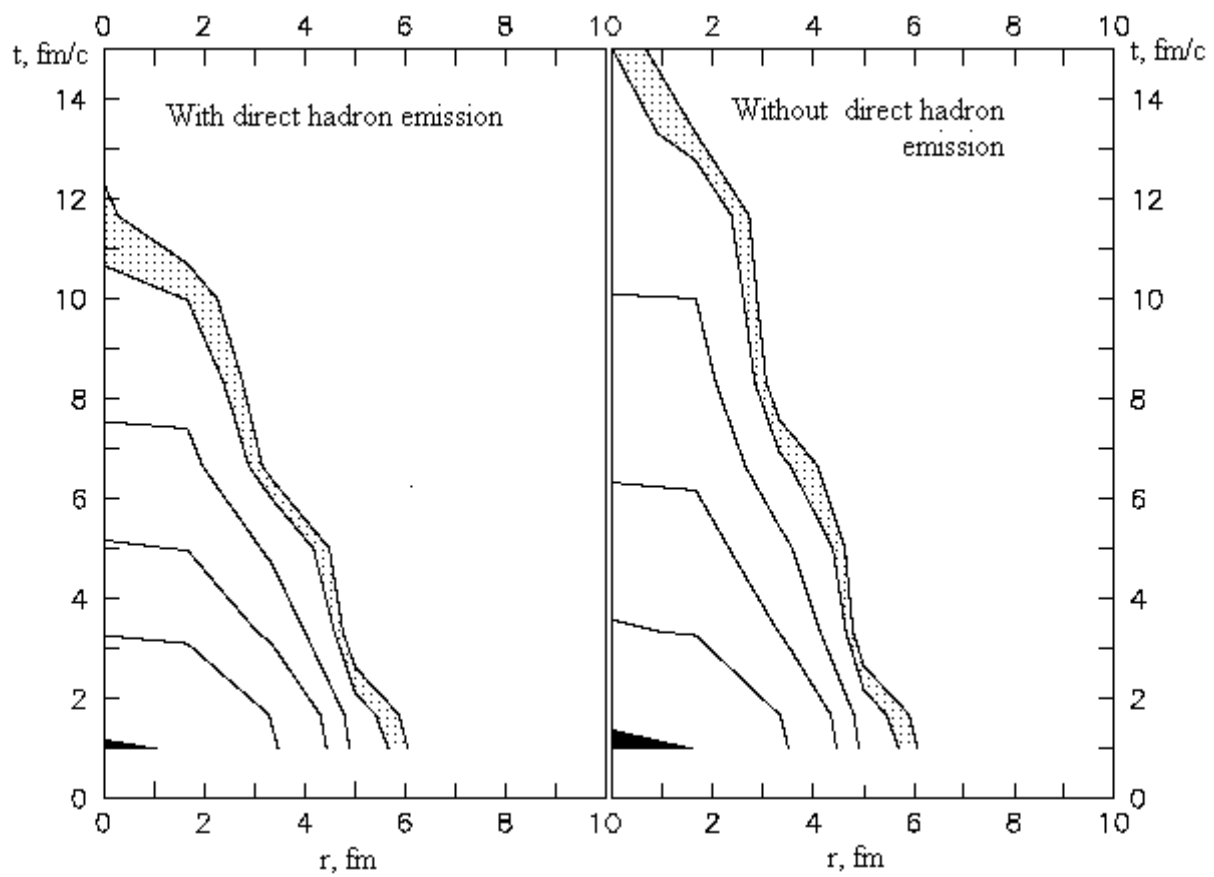


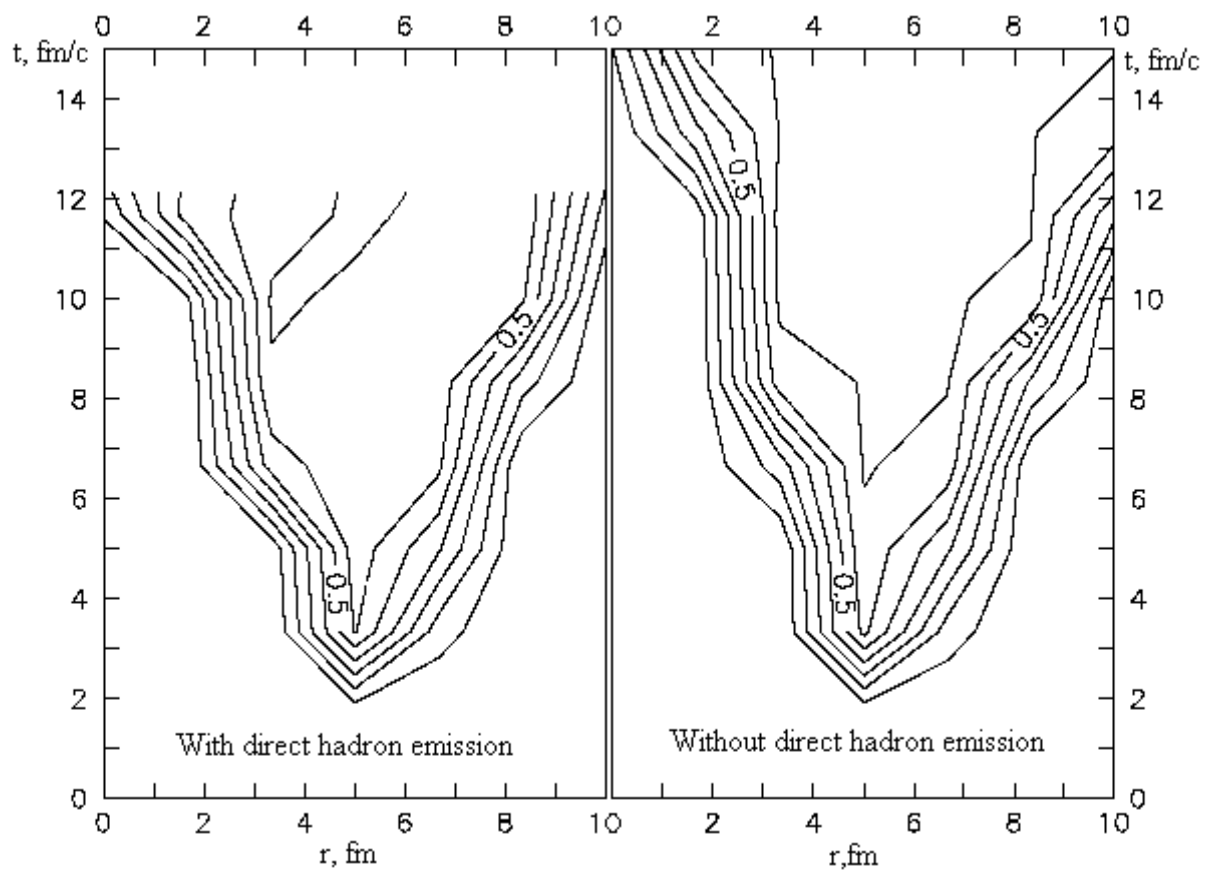
S+Au, 200 AGeV



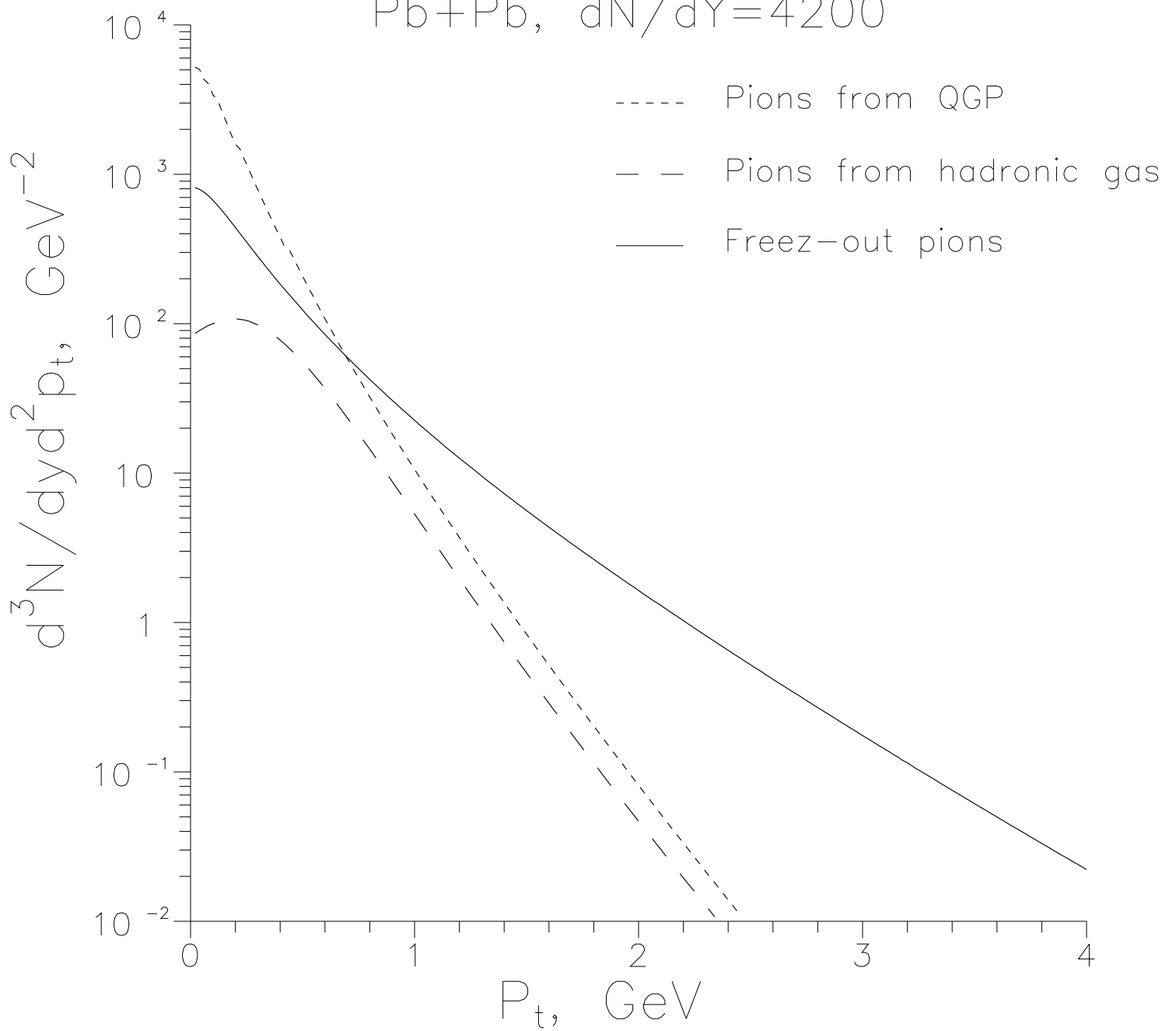


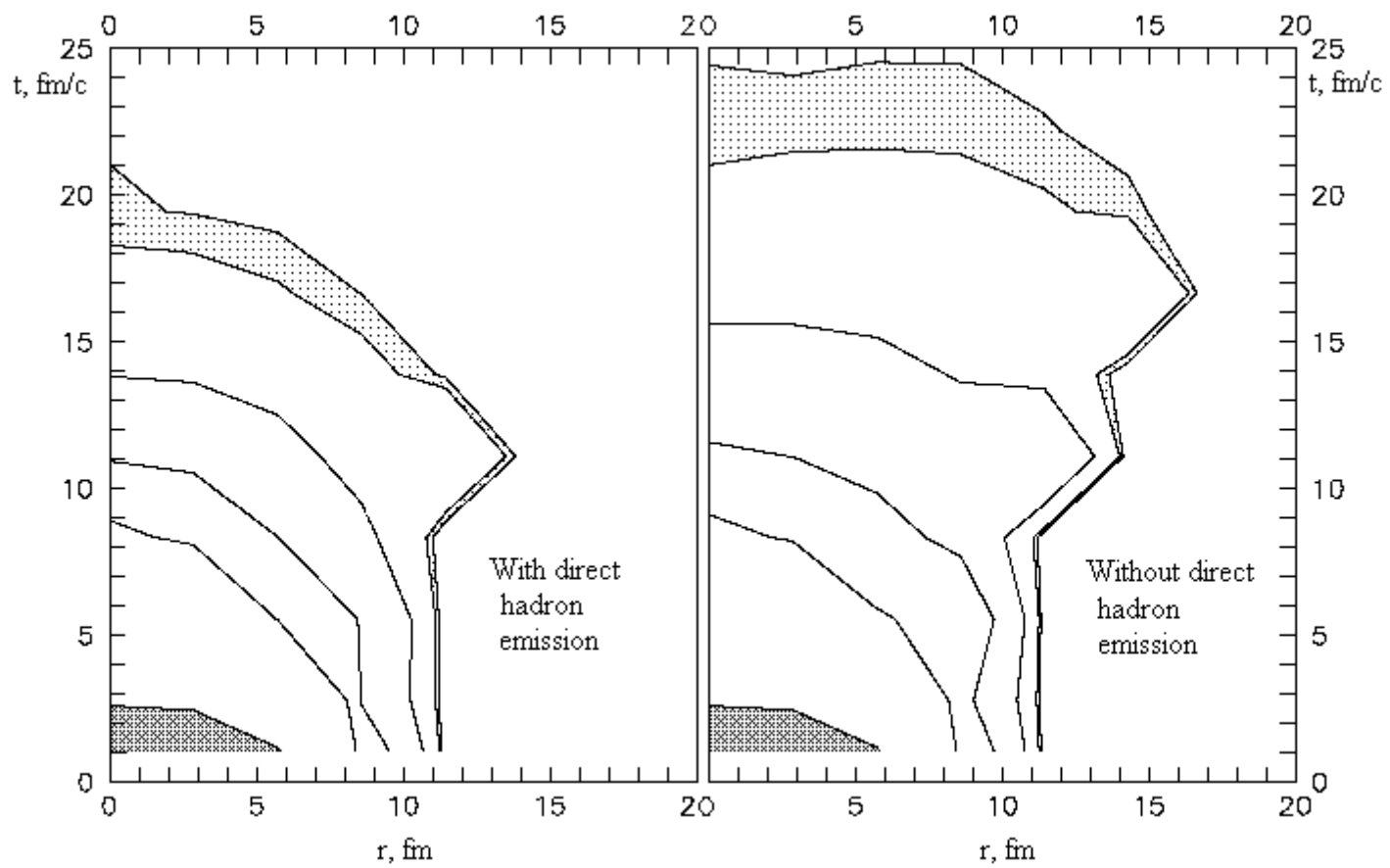




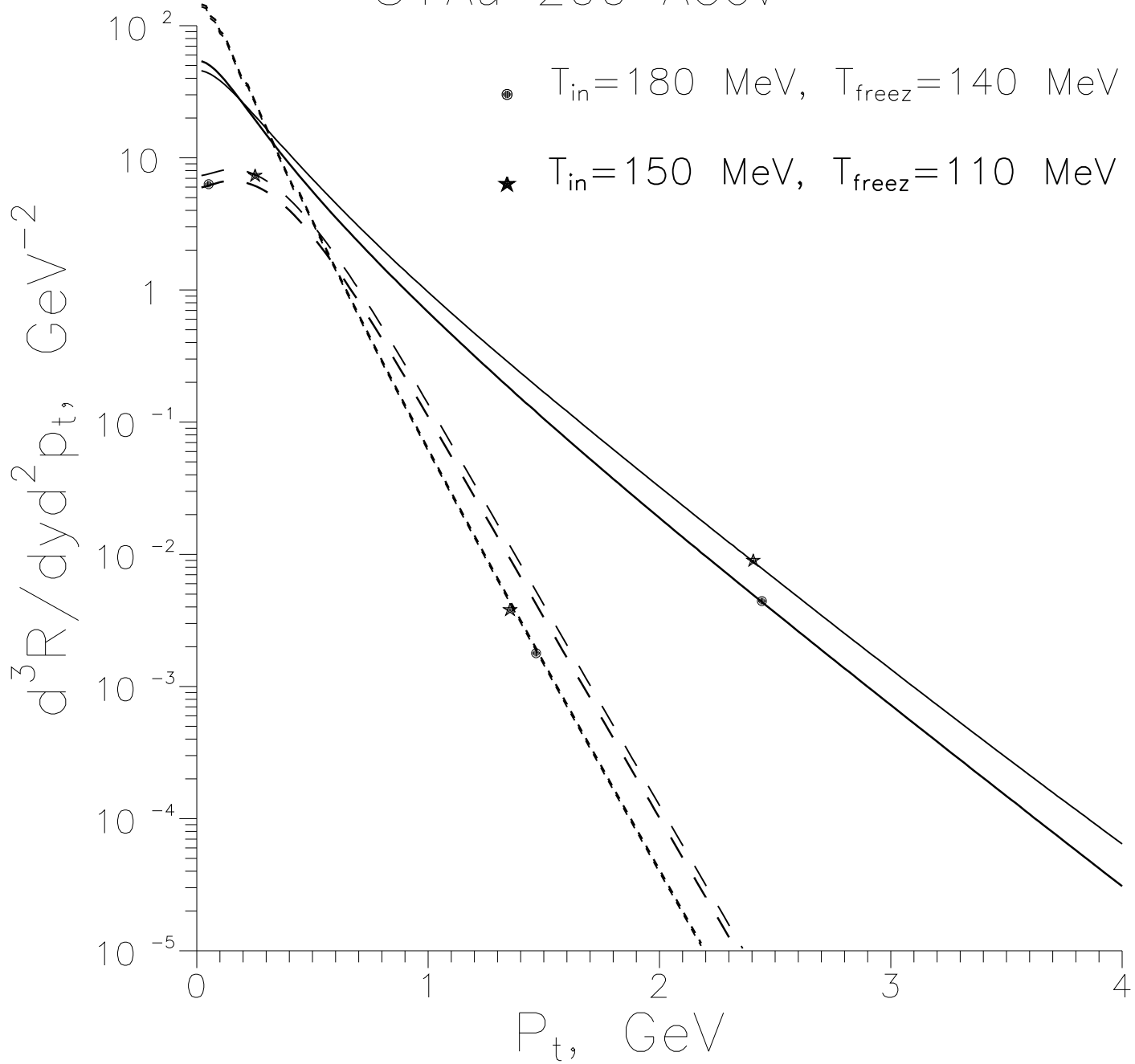


Pb+Pb, $dN/dY=4200$

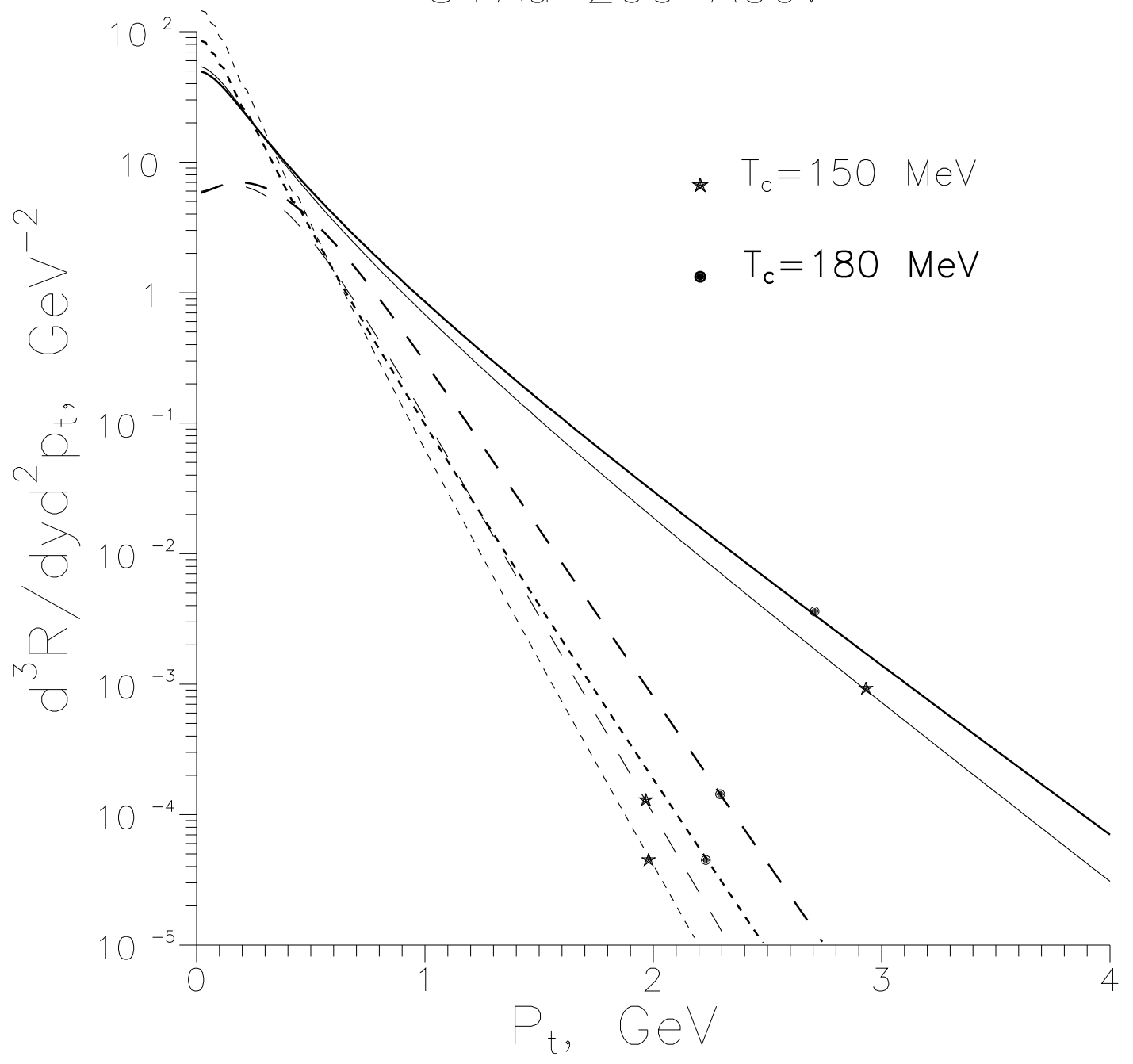




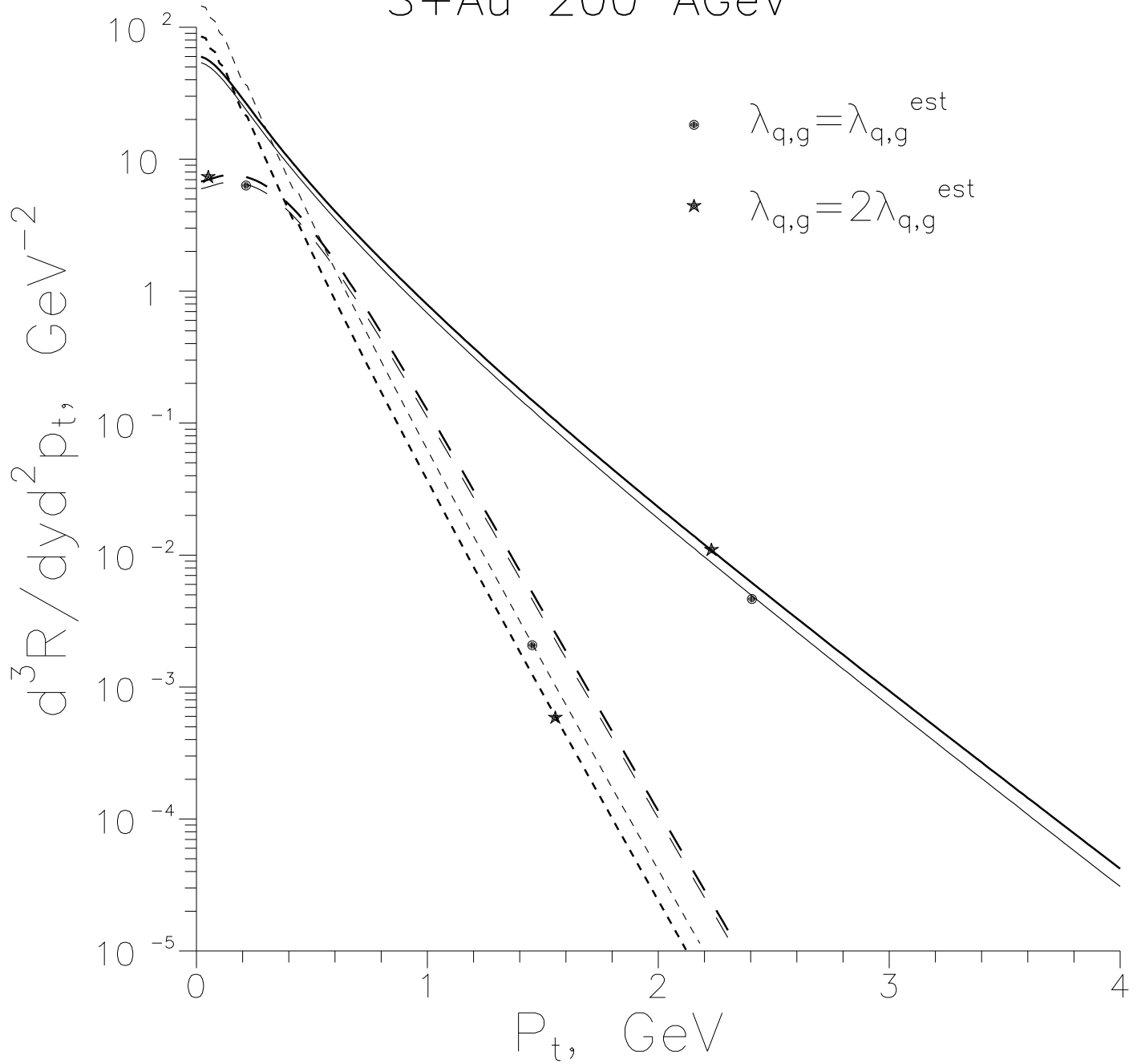
S+Au 200 AGeV



S+Au 200 AGeV



S+Au 200 AGeV



S+Au 200 AGeV

